Charac
Geolog
a Globa
Spaceb

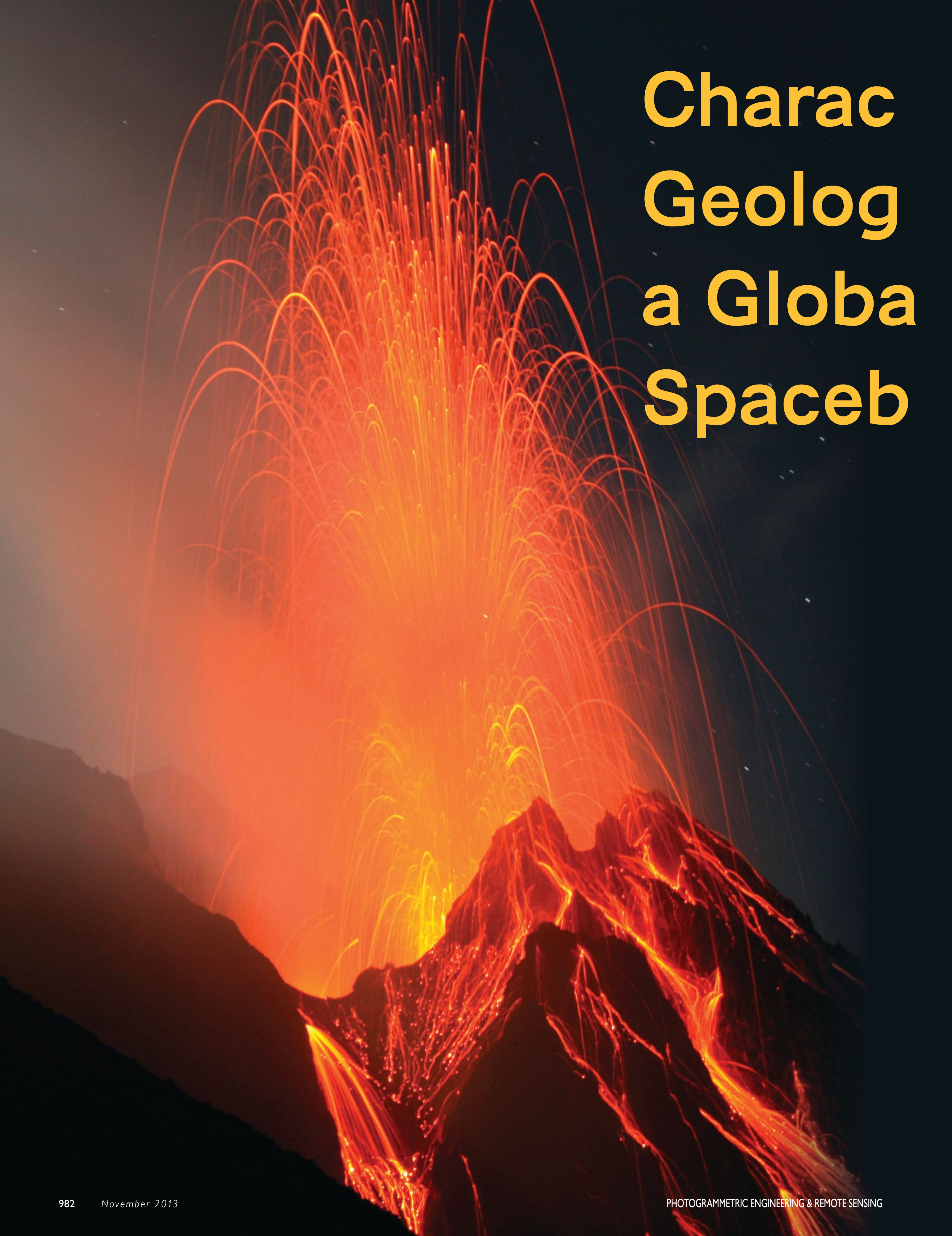

terization of ical Hazards Using lly Observing orne SAR

By Estelle Chaussard and Falk Amelung

Introduction

Geological hazards threaten millions of people living in vulnerable areas worldwide. Monitoring of such hazards can help decision-makers take measures to reduce the associated risks. Ground deformation characterization using satellite-based Interferometric Synthetic Aperture Radar (InSAR), which measures ground displacement in the radar line-of-sight (LOS) direction between passes of a satellite over the same area, can play an important role for hazard assessment and the mitigation of disasters. For example, the arrival of a new magma batch beneath a volcano can be detected by observations of edifice inflation, which can help identify volcanoes that are likely to erupt in the near future (Lu *et al.,* 2007; Segall, 2013). Similarly, land subsidence, which threatens the integrity of buildings and infrastructures and increases the risk of flooding in coastal regions or near rivers, can be precisely mapped with InSAR (Raucoules *et al.,* 2007). Spaceborne monitoring of other geological hazards (not discussed in this paper) includes slow creep and strain accumulation along major faults and catastrophic landslides generally preceded by long-term slow motion.

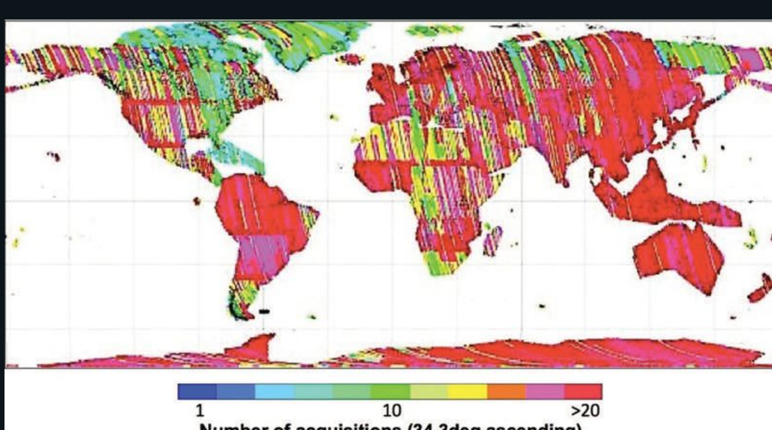

Figure 1. 2006-2011 ALOS PALSAR coverage color-coded according to the number of acquisitions (modified from *JAXA*, 2011).

Opening the Way to Systematic Global-Scale Ground Deformation Monitoring

The Advanced Land Observing Satellite (ALOS) of the Japanese Space Exploration Agency (JAXA) acquired SAR data with global coverage between late 2006 and mid 2011 on a 46-day repeat orbit (Rosenqvist *et al*., 2007). Most of the world's continents were imaged ~15-25 times, leading to the first spatially and temporally consistent global repeat SAR dataset (Figure 1).

Because the PALSAR sensor onboard ALOS was L-band (wavelength of 23.6 cm), it enabled measurements through vegetation, soil, sand, and even dry snow (Sandwell *et al.,* 2008; Dall, 2007) environments in which shorter-wavelength SARs measurements (X- or C-band) are limited by temporal decorrelation of the radar signal. ALOS InSAR time-series, which precisely track ground deformation between the first and the last acquisition (Berardino *et al*., 2002), enables cm-scale ground deformation mapping worldwide, including in populated areas of countries with emerging economies prone to land subsidence and in the Pacific Ring-of-Fire, which comprises most of the world's dangerous explosive volcanoes. In contrast, previous satellites acquired temporally dense data sets mostly over Europe where they have been extensively used to generate time-series measurements (Terrafirma, 2009; Tele-Rilevamento Europa, 2011; Italian National Geoportal, 2013).

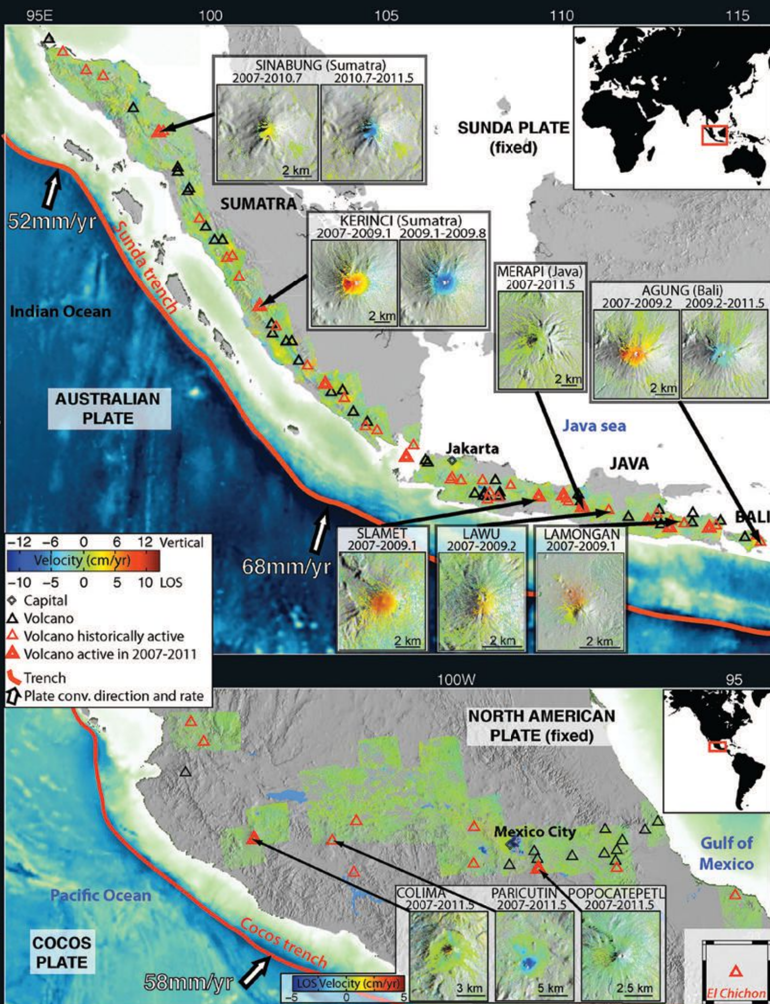

Figure 2. ALOS InSAR ground velocity maps of the Indonesian (top) and Mexican (bottom) volcanic arcs. Uplift is shown in red and subsidence in blue. Insets: volcanoes with deformation or no deformation but unrest periods (Merapi, Popocatépetl, and Colima). 2007-2011 ALOS data was used at four Indonesian volcanoes (Sinabung, Kerinci, Merapi, and Agung, upper side) and on the Mexican arc. The other Indonesian volcanoes were monitored with 2007-2009 ALOS data. Inflation prior to eruption was detected at Sinabung and Kerinci in Sumatra (showing also post-eruptive deflation) and at Slamet in Java. Inflation episodes at the other volcanoes were not followed by eruptions.

With respect to the ground deformation they generate, we can distinguish two types of volcanic systems (Chaussard *et al.,* 2013). The first type, closed volcanic systems, is characterized by inflation of the edifice prior to an eruption due to significant pressurization of its magma reservoir. This inflation is readily detected by InSAR and represents the first stage of volcanic unrest. If the reservoir pressure overcomes the strength of the wall rock, the wall breaks and magma propagates to the surface. The removal of materials from the reservoir during an eruption causes deflation of the edifice. Such a cycle occurred at Sinabung in Indonesia associated with its 2010 eruption (Figure 3, a), whereas at Agung, the inflation was not followed by an eruption, indicating that the pressure remained below the strength of the wall rock and that the magma supply stopped (Figure 3, b). Understanding whether inflation will lead to an eruption is an area of active research and requires observations over multiple deformation cycles. The second type, open volcanic systems, does not show edifice-wide inflation prior to an eruption because a semi-permanent conduit links the reservoir to the surface, impeding its pressurization. The regularly active volcanoes Colima and Popocatépetl in Mexico and Merapi in Indonesia are part of this category. At open volcanic systems, SAR amplitude images can be used instead of phase images to monitor landform changes during volcanic crises, such as the extrusion and deformation of lava domes (Pallister *et al.*, 2012).

Volcanic Hazards

We have used ALOS's global ground deformation monitoring capability to perform systematic surveys in western Indonesia and central Mexico covering areas of 600,000 and 200,000 km^2, respectively. The survey of the Indonesian volcanic arc reveals conclusive evidence that six volcanoes inflated during a 2-year period (Figure 2, top). Three of these volcanoes erupted afterwards (Chaussard and Amelung, 2012), demonstrating that space-derived ground deformation data, if obtained on a routine basis, could contribute to the early warning of volcanic unrest and guide the deployment of ground-based equipment to track magma movements below the surface. The survey of the Mexican volcanic arc shows no signs of volcanic inflation (Figure 2, bottom). However, a comparison between the two regions provides insight into the potential and limitation of using InSAR as a forecast tool.

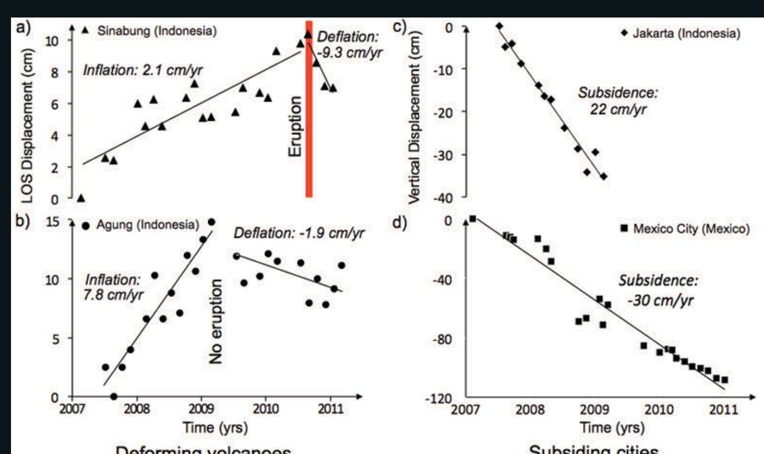

Figure 3. LOS (a and b) and vertical (c and d) displacement time series at two Indonesian volcanoes (a and b): Sinabung in Sumatra (a, black triangles) and Agung in Bali (b, black circles) and in the capitals of Indonesia and Mexico (c and d): Jakarta (c, diamonds) and Mexico City (d, squares). The black lines show the best-fitting linear regressions with the corresponding deformation rates. The red vertical bar marks the eruption of Sinabung, which coincided with the end of the inflation period. On the opposite, at Agung no eruption followed the observed inflation period.

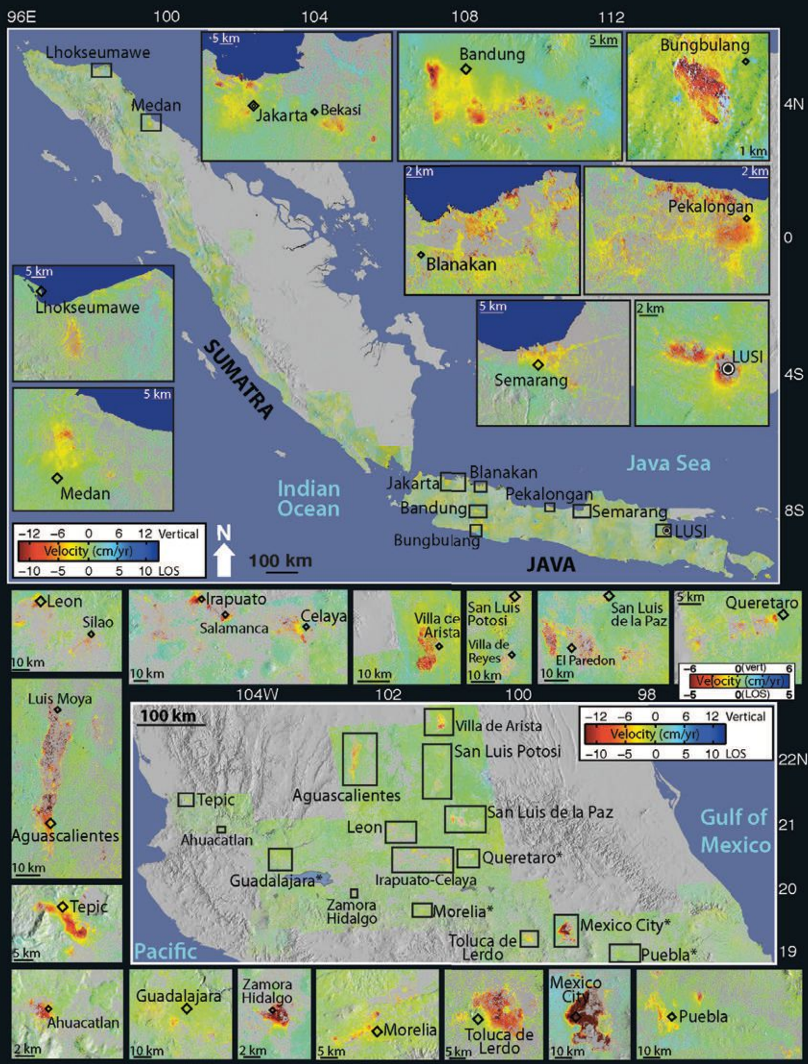

Figure 4. 2007-2009 ALOS InSAR ground velocity map in Indonesia (top) and 2007-2011 velocity map in central Mexico (bottom). The subsiding areas appear in red and are marked by black rectangles, which are zoomed-in in the insets (with a smaller color scale in Mexico). LUSI is the Indonesian mud volcano erupting since 2006. In Mexico asterisks mark the sites on the UNESCO World Heritage list.

Land Subsidence Hazards

The same regional surveys also allowed us to identify and monitor land subsidence with high spatial and temporal resolution. In Indonesia nine subsiding areas were detected, including six major cities, only three of which were previously reported (Figure 4, top; Chaussard *et al.,* 2013). Land subsidence is mostly caused by groundwater extraction for industrial use and is particularly rapid in the capital of Jakarta, where it reaches over 20 cm/yr (Figure 3, c). If subsidence continues at these rates, densely populated coastal areas will be below sea level within a few decades. About 35% of Jakarta is at an elevation of 5 m above the current sea level and is subsiding at 8 cm/yr on average. At this rate, it will take only 60 years until this part of the city is below the current sea level, or even less considering the sea level rise related to the melting of ice sheets and glaciers.

In central Mexico we identified a total of 21 subsiding areas, mostly located in major cities (Figure 4, bottom; Chaussard *et al.*,), only seven of them were previously reported. The fastest subsidence, up to 30 cm/yr, occurs in the capital of Mexico City (Figure 3, d). Similar to the situation in Indonesia, subsidence is largely caused by groundwater extraction but mostly for agricultural and urban use. In Mexico, preexisting faults typically limit subsiding areas, resulting in strong differential, which threatens the integrity of buildings, endangering the population and menacing UNESCO World Heritage sites (Figure 4, bottom).

Hazards associated with land subsidence in both locations also include a decrease in water access and quality. Models of aquifer compaction and groundwater flow based on the InSAR derived subsidence maps could lead to a better characterization of the aquifer dynamics (Hoffmann *et al.*, 2001) and to a more sustainable groundwater use at regional scales.

Requirements for Future Hazards-Dedicated SAR Missions

Our studies highlight the value of continuously observing spaceborne SAR systems. The global ALOS archive offers an opportunity for worldwide assessment of geological hazards using InSAR time-series.

Future missions with geohazard objectives should follow the ALOS example and strive to acquire repeated imagery over the continents with unchanged viewing geometry and homogeneous temporal spacing. A shorter repeat period than the 46 days of ALOS would resolve short-term volcanic inflation prior to eruptions and would lead to a better measurement accuracy, enabling the study of tectonic hazards by measuring elastic strain accumulation along seismogenic faults.

The European Sentinel-1 constellation (scheduled to launch in 2014) will provide 6-12 day repeat coverage; however, its value for monitoring tropical volcanoes remains to be seen because of the use of a C-Band radar sensor. The U.S. and German-Japan mission concepts, planned for the end of this decade (DESDYnI and Tandem-L, respectively), should provide the high-temporal (weekly or shorter repeat period) and high-spatial resolution imagery needed to advance the assessment of geological hazards.

Acknowledgements

These studies were supported by the National Aeronautics and Space Administration (NASA). The ALOS-PALSAR data are copyrighted by the Japanese Space Agency (JAXA) and the Japanese Ministry of Economy, Trade and Industry (METI) and were made available by the U.S. Government Research Consortium (USGRC) through the Alaska Satellite Facility (ASF).

References

Berardino, P., G. Fornaro, R. Lanari, & E. Sansosti, 2002. A new algorithm for surface deformation monitoring based on small baseline differential SAR interferograms, *IEEE Transactions on Geoscience and Remote Sensing*, *40*(11), 2375–2383, doi:10.1109/TGRS.2002.803792.

Chaussard, E., & F. Amelung, 2012. Precursory inflation of shallow magma reservoirs at west Sunda volcanoes detected by InSAR, *Geophysical Research Letters*, *39*(21), L21311, doi:10.1029/2012GL053817.

Chaussard, E., F. Amelung, H. Abidin, & S.-H. Hong, 2013. Sinking cities in Indonesia: ALOS PALSAR detects rapid subsidence due to groundwater and gas extraction, *Remote Sensing of Environment*, *128*, 150–161, doi:10.1016/j.rse.2012.10.015.

Chaussard, E., F. Amelung, & Y. Aoki, 2013. Characterization of open and closed volcanic systems in Indonesia and Mexico using InSAR time series, *Journal of Geophysical Research-Solid Earth*, n/a–n/a, doi:10.1002/jgrb.50288.

Dall, J., 2007. InSAR elevation bias caused by penetration into uniform volumes, *Geoscience and Remote Sensing, IEEE Transactions on*, *45*(7), 2319–2324, doi:10.1109/TGRS.2007.896613.

Hoffmann, J., H.A. Zebker, D.L. Galloway, & F. Amelung, 2001. Seasonal subsidence and rebound in Las Vegas Valley, Nevada, observed by synthetic aperture radar interferometry, *Water Resources Research*, *37*(6), 1551-1566.

Japan Aerospace Exploration Agency (JAXA), 2011. PALSAR data archives, Presentation at the PIXEL workshop, Kyoto University Dec. 2011.

Lu, Z., D. Dzurisin, C.W. Wicks, Jr., J.A. Power, J. Kwoun, & R. Rykhus, 2007. Diverse deformation patterns of Aleutian volcanoes from satellite interferometric synthetic aperture radar (InSAR), in J. Eichelberger, E. Gordeev, P. E. Izbekov, M. Kasahara, & J. Lees, Eds.,*Volcanism and Subduction, AGU Monograph Series*, *172*, 249–261, doi:10.1029/172GM18.

Italian National Geoportal, 2013. Progetto Persistent Scatterers Interferometry, http://www.pcn.minambiente.it/GN/progetto_psi.php?lan=en (accessed 23 August 2013).

Pallister, J.S., D.J. Schneider, J.P. Griswold, R.H. Keeler, W.C. Burton, C. Noyles, C.G. Newhall, and A. Ratdomopurbo, 2012. Merapi 2010 eruption—Chronology and extrusion rates monitored with satellite radar and used in eruption forecasting, *Journal of Volcanology and Geothermal Research*, 1–9, doi:10.1016/j.jvolgeores.2012.07.012.

Raucoules, D., C. Colesanti, & C. Carnec, 2007. Use of SAR interferometry for detecting and assessing ground subsidence, *Comptes Rendus Geosciences*, *339*(5), 289–302, doi:10.1016/j.crte.2007.02.002.

Rosenqvist, A., M. Shimada, N. Ito, & M. Watanabe, 2007. ALOS PALSAR: A Pathfinder mission for global-scale monitoring of the environment, *Geoscience and Remote Sensing, IEEE Transactions on*, *45*(11), 3307–3316, doi:10.1109/TGRS.2007.901027.

Sandwell, D.T., D. Myer, R. Mellors, M. Shimada, B.A. Brooks, & J. Foster, 2008. Accuracy and resolution of ALOS interferometry: Vector deformation maps of the Father's Day intrusion at Kilauea, *IEEE Transactions on Geoscience and Remote Sensing*, *46*(11), 3524–3534, doi:10.1109/TGRS.2008.2000634.

Segall, P., 2013. Volcano deformation and eruption forecasting, *Geological Society, London, Special Publications*, doi:10.1144/SP380.4.

Tele-Rilevamento Europa, 2011. Regional Mapping, Retrieved from http://treuropa.com/natural-hazards/regional-mapping/.

Terrafirma, 2009. The Terrafirma Atlas, terrain motion across Europe, A compendium of results produced by the European Space Agency, GMES Service Element project Terrafirma 2003-2009. Retrieved from http://esamultimedia.esa.int/multimedia/publications/TerrafirmaAtlas/pageflip.html.

Authors

Estelle Chaussard
Department of Earth and Planetary Science
University of California, Berkeley
Berkeley, CA 94720-4767, USA
School of Marine and Atmospheric Science
University of Miami
Miami, FL 33149-1098, USA

Falk Amelung
School of Marine and Atmospheric Science
University of Miami
Miami, FL 33149-1098, USA